Optical and UV Sensing Sealed Tube Microchannel Plate Imaging Detectors with High Time Resolution

Oswald H. W. Siegmund, John V. Vallerga, Anton S. Tremsin, Jeffrey Hull
Space Sciences Laboratory, U.C. Berkeley
Anil U. Mane, Jeffrey W. Elam
Argonne National Laboratory, Lemont, Il
Aileen O'Mahony
Incom Inc., Southbridge, MA

ABSTRACT

Imaging photon counting sensors, with high timing resolution, using GaAs and Super-GenII photocathodes have been developed. These 18 mm active area format sensors with microchannel plates and cross strip anode readouts in combination with high speed event processing electronics can process high event rates (5 MHz with 82% livetime), and support local area counting rates of ~40 kHz (100 μm spot). For GaAs the peak quantum efficiency is ~30% (@ 560 nm) with spatial resolution of ~40 μm FWHM (~ 10^6 gain) and event timing resolution of ~260 ps (FWHM). For Super-GenII the peak quantum efficiency is ~20% with spatial resolution of <30 μm FWHM (~6 x10^5 gain) and event timing resolution of <100 ps (FWHM). We have also used novel microchannel plates that have been constructed with borosilicate microcapillary arrays and activated by atomic layer deposition. Examples have been incorporated into sealed tubes for evaluation. One trial uses an opaque GaN photocathode deposited onto these microchannel plates in a tube with a cross delay line readout. This device achieves ~40 μm spatial resolution, and its gain increased by an order of magnitude during the tube processing to achieve a uniform stable level. A 50mm Planacon was also constructed using atomic layer deposited microchannel plates, and this achieves standard bialkali quantum efficiency levels and has been used to detect fast laser pulse signals.

Keywords: Microchannel plate, GaAs, GaN, photon counting, imaging, timing

1. INTRODUCTION

Microchannel plate (MCP) photon counting, event timing, imaging detectors have found wide use in astronomical [1-6], remote sensing [7], and biological imaging [8, 9] applications. Many readout configurations are possible, however we have successfully employed a cross strip (XS) anode which senses microchannel plate charge signals on two orthogonal layers of strips and uses charge division and centroiding of the charge distribution to encode event X-Y positions. An XS sealed tube detector scheme is shown in Fig. 1. Light passes through the input window and is converted to photoelectrons by a photocathode. Photoelectrons are emitted and then amplified by a pair of MCPs and then sensed by a readout anode that has two orthogonal sets of conductive strips. Sealed tube configurations (Fig.2) with proximity focus GaAs photocathodes [10] and Super-GenII [11] have been developed for visible light sensing. These use a pair of 6 μm pore MCPs with gains up to ~10^6 and 22 mm format XS anodes with an active area of 18 mm (Fig. 3). The GaAs photocathodes provide quantum efficiency of ~30% in the 550 nm to 850 nm region, while the Super-GenII achieves ~20%. In combination with a second generation of Parallel Cross Strip (PXS-II) electronics we have evaluated the 18mm sealed tube XS detectors, demonstrating high spatial resolution (~30-40 microns FWHM), input event rates of >5 MHz, and event timing as good as ~100 ps FWHM. Good spatial imaging and gain uniformity have also been achieved at low MCP gain (10^6). Background rates are predominantly due to the thermionic noise of the photocathodes, which can be controlled by modest cooling to ~0°C.

Sealed tube detectors have also been constructed using MCPs [12] made by atomic layer depositions (ALD) on borosilicate micro-capillary arrays. ALD MCPs have many performance characteristics typical of conventional microchannel plates [12], however in some areas they show marked improvements. ALD MCPs have low intrinsic background (<0.06 events cm^{-2} s^{-1}) and can have high stability, with no gain decreases over at least 7 C cm^{-2} of charge extraction [13] after a vacuum bake process. ALD MCPs have been used in a PHOTONIS Planacon 32 x 32 anode device, and in a sealed tube 25mm detector with a cross delay line readout. The latter also has a GaN opaque photocathode deposited onto the front MCP, and showed a factor of 10 increase in gain during its vacuum baking step. The performance of these two devices and their implications will be discussed.

2. CROSS STRIP SEALED TUBE DETECTORS

Imaging MCP sealed tubes with XS readout and Super-GenII and GaAs photocathodes have been made for high time resolution, photon counting, imaging applications [10, 11]. Significant improvements to the readout electronics [14] have been made since our initial evaluations of these devices, and have now enabled more detailed performance investigations to be done. We review the details of the design, and then present efficiency, photon imaging and uniformity, and timing results.

2.1 Cross Strip – Sealed Tube Microchannel Plate Detectors

For sealed tube ultra high vacuum devices we have implemented the 22 mm XS anode as a robust multi-layer metal and ceramic structure on an alumina substrate (Fig. 3). The strip conductor-set for each axis has a ~0.6 mm period with ~ 50% of the charge impinging on each orthogonal set. Each strip signal is connected by a hermetic via to the back of the anode. A fan out outside the vacuum accommodates a standard connector to the amplifier electronics (Fig. 4). The XS anodes are set ~2.5 mm behind the MCP stack, and the MCP-anode gap voltage is adjusted so that charge is collected on several neighboring fingers (Fig. 1) to obtain optimal event position centroiding [11]. Two 6 μm pore 80:1 l/d MCPs provide sufficient electron gain (~ 10^6) for high resolution imaging and timing. The window-MCP gap is small (<200 μm) and the bias is adjusted to optimize the transit time spread and event timing performance.

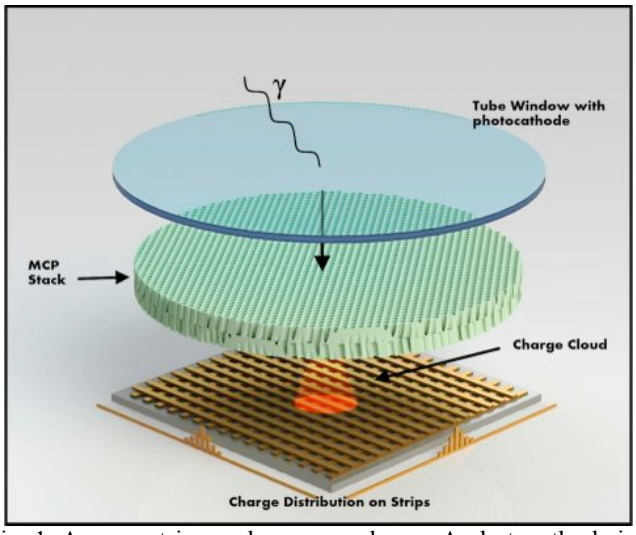


Fig. 1. A cross strip anode sensor scheme. A photocathode is deposited on a window facing a pair of MCPs. Emitted photoelectrons are detected by the MCPs and collected by several strips in each axis of the anode to encode positions.

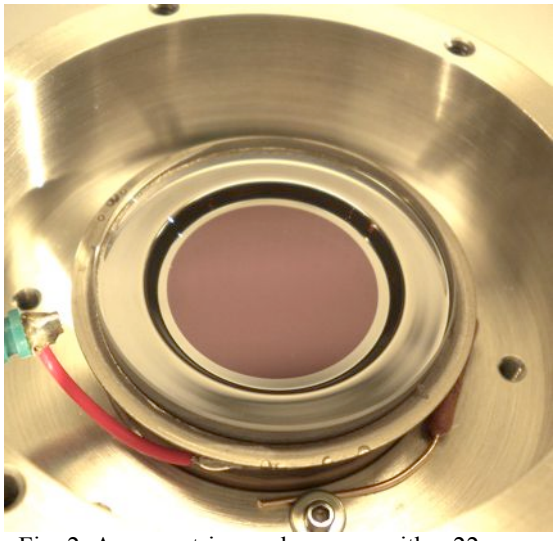


Fig. 2. A cross strip anode sensor with a 22 mm readout anode and a pair of 6μm pore 80:1 l/d MCPs for single photon counting, event timing, imaging, applications. Super-GenII photocathode.

2.2 Sealed Tube Cross Strip Anode Microchannel Plate and Photocathode Performance

Several GaAs and Super-GenII photocathode XS readout sealed tubes (Fig. 2) were fabricated by Photonis-NL using 22 mm XS anodes (Fig. 3). Borosilicate glass entrance windows were used in a proximity focused configuration (<200 μm gap, ~100 Vgap). The response of these tubes (Fig. 5) ranges from ~400 nm to 900 nm with peak values of ~20% for Super-GenII tubes and 30% for GaAs tubes. The thermal noise for the GaAs sealed tubes is high at room temperature (>80 kHz cm^{-2}) and is about an order of magnitude higher than the Super-GenII tubes. However, with active cooling this drops to ~12 kHz cm^{-2} at 8°C for GaAs and <500 Hz cm^{-2} for Super-GenII. The quantum efficiency of several Super-GenII tubes was measured almost 5 years after their original manufacture (Fig.5). This shows no significant change in performance over that time. The pulse amplitude distribution for these tubes (Fig. 6), using pairs of 6 μm pore 80:1 l/d MCPs, is quite good even at the comparatively low gain (4 x 10^5 to 1 x 10^6) which we are able to employ with the XS readout. This low gain is important is achieving high local event rate performance (>20 kHz, [11]).

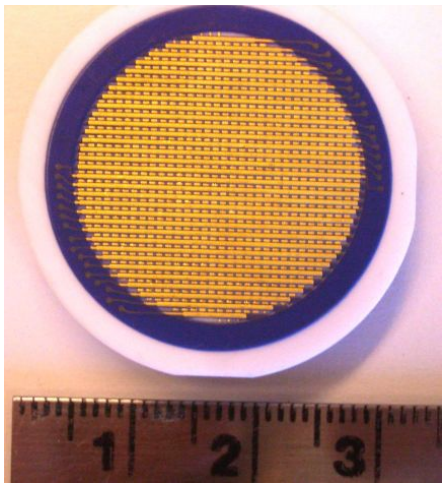


Fig. 3. View of a 22 mm cross strip anode showing the 32 + 32 charge collection strips.

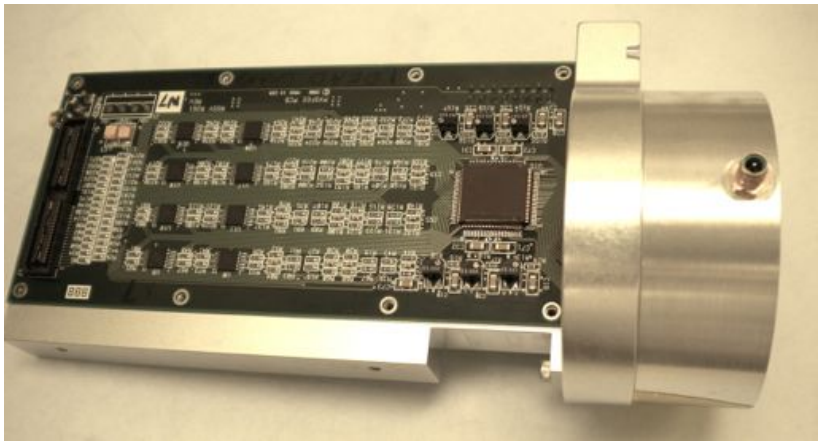


Fig. 4. Housing for cross strip anode sealed tubes, with a front end amplifier board including two 32 channel ASIC preamplifiers

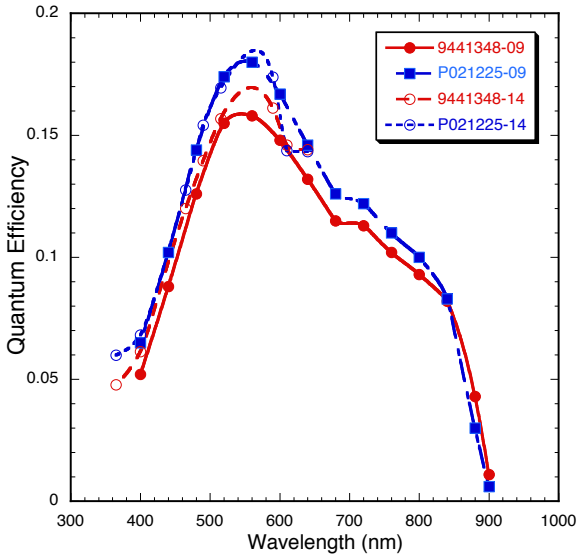


Fig. 5. Photocathode quantum efficiency for two 18 mm sealed tube cross strip anode detectors (Super-GenII cathodes) measured in 2009 and again in 2014.

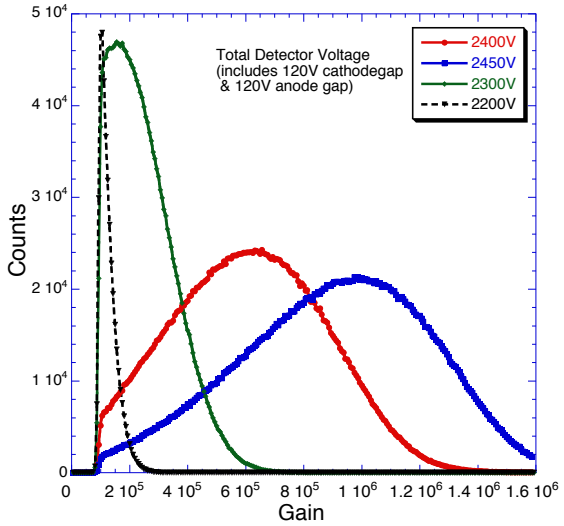


Fig. 6. Single photon signal pulse amplitude distributions for an 18 mm sealed tube Super-GenII cross strip anode sensor at various gain levels.

2.3 Cross Strip Sealed Tube Detector System Imaging Tests

The overall imaging performance of the sealed tube 18mm XS sensors combined with the electronics, consisting of the PXS-II and the RD20 amplifier board (Fig. 4) was investigated. Measurement of the spatial resolution and image linearity accomplished with test mask images for the Super-GenII tubes and GaAs tubes was previously reported [10, 11]. The resolution reaches ~40 µm (FWHM) for GaAs tubes and ~30 µm (FWHM) for the Super-GenII tubes. The width of the bright spot in Fig. 7, with a Super-GenII tube gives a 26 µm FWHM resolution point spread function.

The overall image response uniformity in both sealed tube types is dominated by residual banding in both X and Y. This is attributable to centroid calculation errors due to charge sharing errors between individual strips and the performance variations of individual amplifiers. This fixed pattern noise is stable and is generally less than ~7%, and standard flat field data sets can be used to correct the non-uniformities. A typical map of average gain for these XS sealed tubes is shown in Fig. 8. The global gain variation is generally less than 10%, however faint features, like the hexagonal modulation due to MCP multifibers can also be seen (Fig. 8).

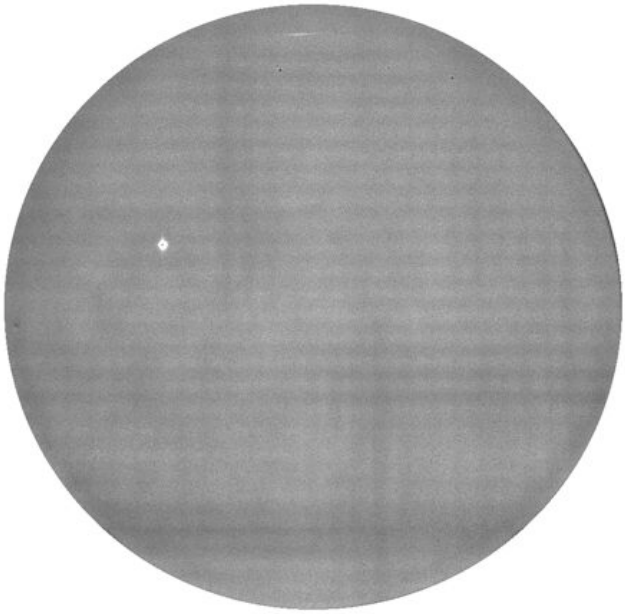


Fig. 7. 22mm cross strip anode sensor with Super-GenII cathode. Uniformly illuminated image shows some anode striping at ~7% modulation and one hot spot. 6 x 10^5 gain

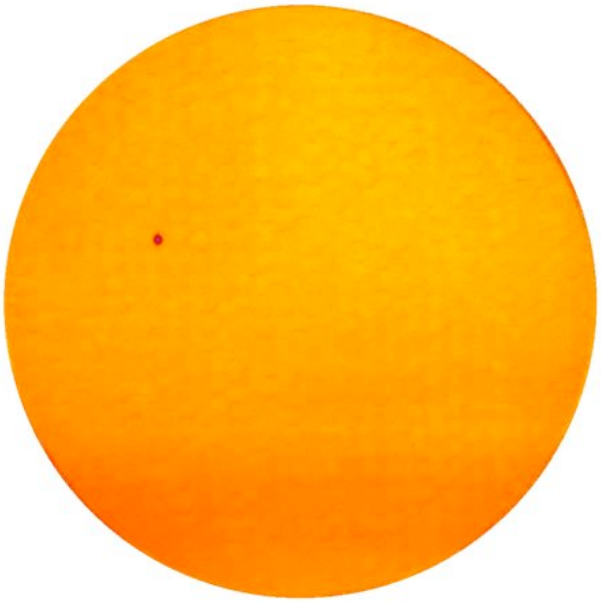


Fig. 8. 22mm cross strip anode sensor with Super-GenII cathode. Gain map image has less than 10% variations, and also shows a faint hexagonal MCP modulation.

2.4 Cross Strip Detector Event Rate and Time Tagging Performance

The count rate throughput of a cross strip readout MCP detector is defined by a global rate limit determined by the event processing electronics system, and a local rate limited by the MCP pore recharge time. We have previously shown [14] that the livetime (paralyzable) of the PXS-II electronics is ~ 82% event throughput at an input rate of 5 MHz. The local rate capability of an MCP detector is limited by the ability of the MCP pores to recharge between events. This is a function of the MCP resistance, the area illuminated and the total charge gain of the MCP stack. Prior measurements [11] have established rates of up to ~40 kHz in small areas (100 µm) with an MCP stack having 60 MΩ resistance. One of the current GaAs XS sealed tubes has a 20 MΩ MCP stack and is capable of a proportionately higher local count rate.

The photon event time-tagging requirements for various applications [7, 8, 9, 11] range from milliseconds in Astronomy, to <100 ps for LIDAR and biological fluorescence lifetime imaging. The 50 MHz sampling frequency of the PXS-II electronics can record a course time stamp of ~20 ns [14], which is sufficient for some of the applications. The high precision timing for more demanding applications can be established with an additional timing channel using the signal at the output face of the MCP stack. A high bandwidth preamplifier (Ortec VT120) was coupled to the bottom of the MCPs. These signals were detected by a Time to Digital converter with a constant fraction input discriminator having ~25 ps (FWHM) timing error. The detected events were timed relative to the pulse source input trigger provided by a laser (610 nm pulsed laser, 80 ps pulse width). The same technique has established ~100 ps time resolution for cross delay line readout sealed tube detectors [8]. Laser spots ~400 µm wide were used to illuminate both the GaAs and Super-GenII sealed tubes at a series of positions across the field of view, and event time spectra were taken at several detector gain values.

The bialkali Super-GenII results (Fig. 9) show timing resolution as good as ~100 ps FWHM, which is close to the laser pulse width (80 ps). The GaAs 18 mm cross strip tube timing resolutions are broader (Fig. 10) reaching ~260ps FWHM. This is significantly more than the expected instrumental limits and is probably indicative of the transit time spread in the thicker GaAs photocathode layer. The trend of timing resolution as a function of MCP gain (Fig. 11) is not strong, but shows a decrease to about 100 ps for the Super-GenII at the higher gains. For GaAs there is little change with gain. Moving the laser spot across the detector area produces little change (Fig. 12) in the timing delay of the laser signals. Both the GaAs and Super-GenII sealed tubes show less than 30 ps change as a function of position. Propagation delays in the signals across the 18mm area support this effect would be less than 50 ps.

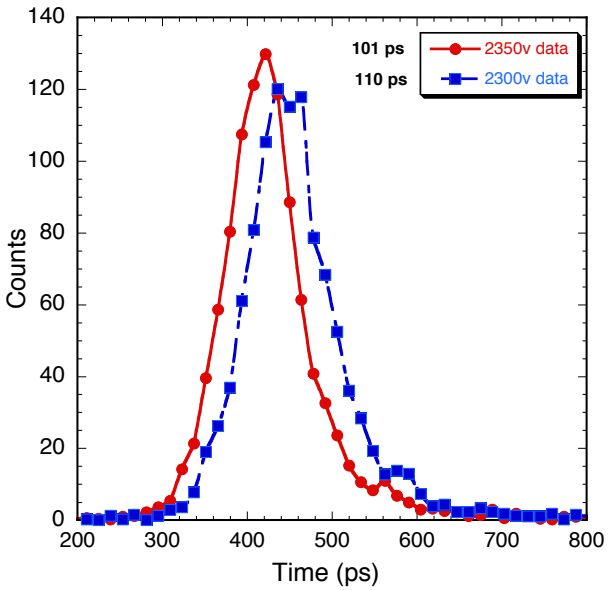


Fig. 9. Event timing error distributions for an 18 mm SuperGenII cross strip sensor system at two MCP gains. Spot illumination, 80 ps 610 nm laser, 120 V cathode gap.

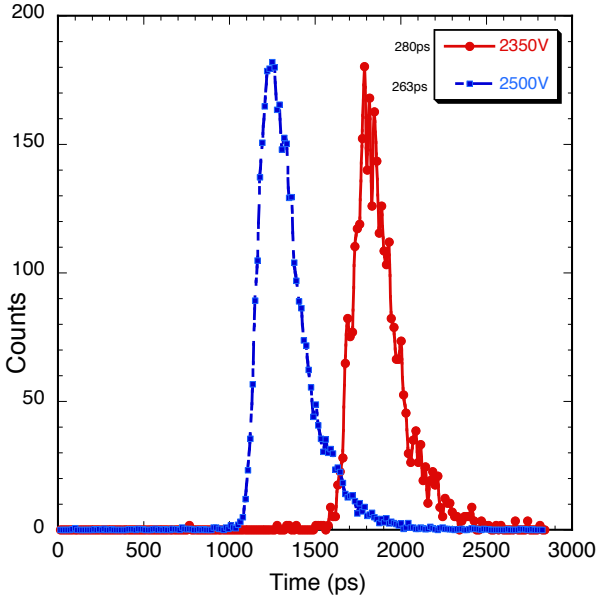


Fig. 10. Event timing error distributions for an 18 mm GaAs cross strip sensor system at two MCP gains. Spot illumination, 80 ps 610 nm laser, 120 V cathode gap.

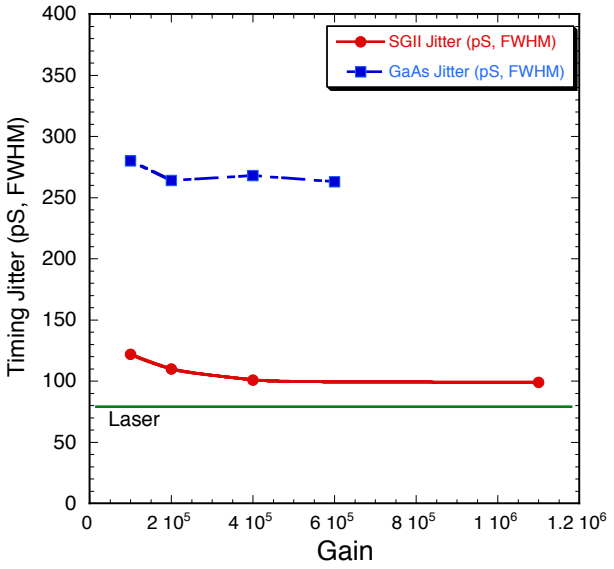


Fig. 11. Event timing jitter for single photon detections vs. gain. 80ps laser spot and 120V window-MCP gap bias. Super-GenII (SGII) and GaAs cross strip sensor systems.

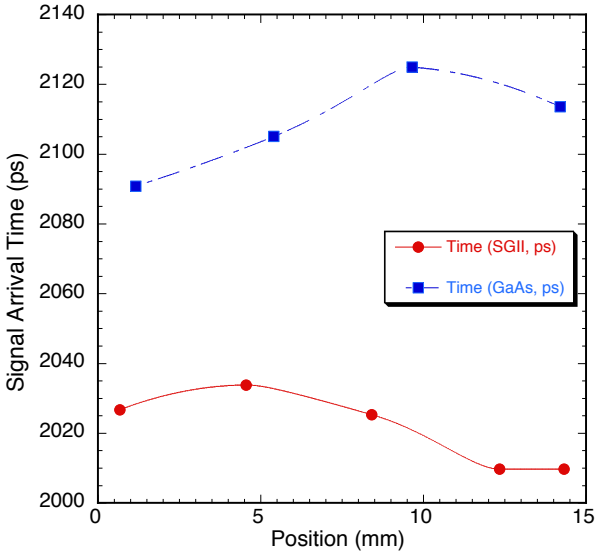


Fig. 12. Timing shift vs position of the laser spot. 80ps laser spot and 120V window-MCP gap bias. Both tube cathode types have ~ 30 ps variation.

3. DEVELOPMENT OF ALD MCP SEALED TUBES AND GaN PHOTOCATHODES

Most sealed tube devices have active areas less than about 5 cm and use either conventional microchannel plates, or dynode multipliers for electron amplification, and are often coupled to coarse pad array readouts [9]. Our collaboration (Large Area Picosecond Photon Detector) consisting of the U. Chicago, Argonne National Laboratory, U.C. Berkeley, U. Hawaii, Incom. Inc., and several other institutions have developed novel ALD borosilicate MCP technologies to realize 20 cm format open face, or sealed tube detectors [12]. The progress on these devices is detailed elsewhere [14]. However, significant achievements have been made in implementing MCPs with borosilicate glass microcapillary arrays coated with resistive and secondary emissive layers using Atomic Layer Deposition [13]. The properties of ALD MCPs make them potentially attractive for sealed tube devices and use with novel photocathode materials. We have begun to explore these capabilities by making a sealed tube with an opaque GaN photocathode (Fig. 13), and a Planacon with ALD MCPs (Fig.14).



Fig. 13. 25 mm sealed tube with a GaN photocathode directly deposited onto a pair of borosilicate substrate ALD coated MCPs (20µm pore, 60:1 l/d). XDL readout.

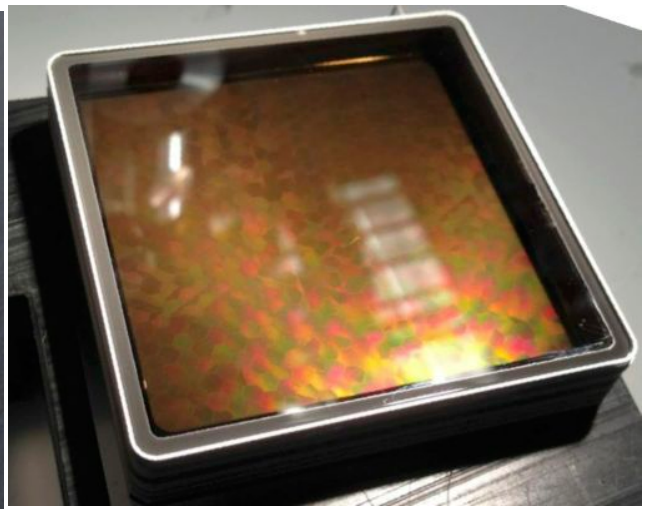


Fig. 14. Planacon sealed tube with a pair of 10 µm pore ALD borosilicate 60:1 MCPs, 32 x 32 anode and Bialkali cathode. 32 x 32 pad readout anode.

3.1 GaN Sealed Tube Construction and Photocathode Development

ALD microchannel plates are based on the concept that a borosilicate micro-capillary array substrate can be made to function as a microchannel plate by deposition of resistive and secondary emissive layers using atomic layer deposition. The process is potentially inexpensive and allows very large microchannel plates to be produced. The glass tube stacking and fusion techniques used are similar to standard MCPs, but no core glass etching is required. ALD deposition of resistive and secondary emissive layers, followed by evaporation of NiCr electrodes complete the MCP fabrication process. Initial tests of the atomic layer deposition technique were performed on 33 mm MCPs [13,15] which showed that many of the performance characteristics are typical of conventional microchannel plates [12]. However, the background rate (~0.06 events cm^{-2} sec^{-1}) is lower than conventional MCPs because the borosilicate glass contains less radioactive alkalis than standard MCP glass formulations. We have also found that in the sealed tube conditioning steps on borosilicate ALD microchannel plates the MCP gain rises by an order of magnitude after a vacuum bake [13]. Furthermore, after this step the MCP gain remained stable [13] during burn-in (to 7 C cm^{-2}).

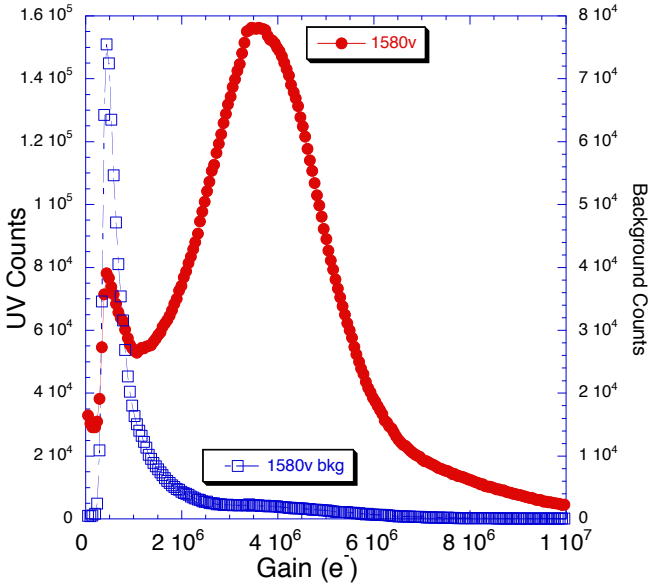


Fig. 15: 25mm GaN ALD MCP sealed tube pulse amplitude distribution with 184nm UV, and background events. GaN coated ALD MCPs (Pair, 20µm pore, 60:1 l/d).

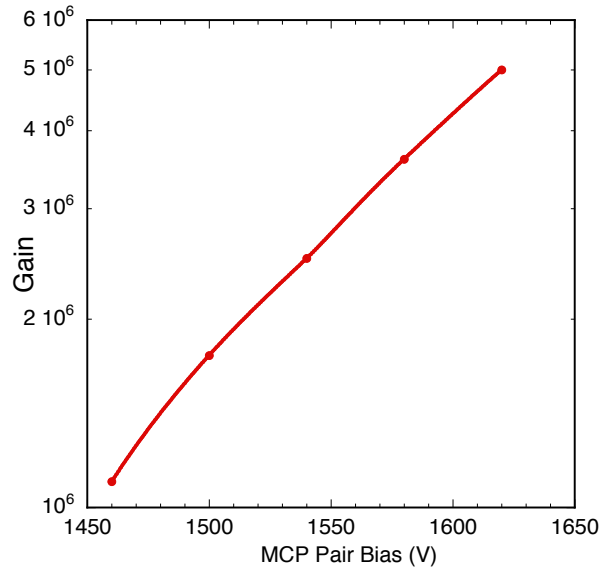


Fig. 16: Gain voltage relationship for GaN coated borosilicate ALD MCPs (20µm pore, 60:1 l/d), in the 25mm sealed tube with cross delay line readout.

A cross delay line readout (25mm) sealed tube design similar to those used previously (Fig. 13) [16] was selected to test the GaN ALD MCPs. This uses a hot indium seal to a magnesium fluoride entrance window to transmit short wavelength UV, and a brazed ceramic/metal vacuum housing. Two 33mm 60:1 l/d, 20 µm pore ALD borosilicate MCPs were chosen to supply gains of $>10^6$. The materials used for these ALD MCPs are capable of sustaining much higher temperatures than standard MCPs. This was advantageous for the deposition (SVT Inc.) of GaN [17] by Molecular Beam Epitaxy onto the top surface of the upper MCP to provide the UV photocathode. The GaN photocathode detector was tested and then processed to seal the tube. Both vacuum bake and MCP "burn-in" were done, and in this case the MCP gain rose about one order of magnitude after undergoing vacuum bake. The "burn-in" was much shorter than a conventional "burn-in". During this short "burn-in" (<0.05 C cm^{-2}) very little gas was observed to be released, and there was no indication of any gain decrease. The final step in tube processing was the window seal, however, prior to this we completed the GaN photocathode activation by deposition of Cs to lower the GaN work function.

The completed sealed tube has a good single photon pulse amplitude distribution (Fig. 15) and an exponential background pulse amplitude spectrum. Gains up to ~5 x 10^6 were achieved (Fig. 16) at quite low overall MCP bias (~800V per MCP) after the gain increase during vacuum bake. The borosilicate ALD MCPs used were from a fairly early development batch and show significant hexagonal multifiber modulation in the accumulated photon counting 2D images (Fig. 17). Another problem was that these MCPs had undergone significant handling before being used for this application and the dust/debris on them resulted in hotspots and deadspots in the images. Some of these features can be clearly seen in high resolution images (Fig. 18) showing the multifiber edges for both MCPs in the stack. Some of the hotspots are small and demonstrate the resolution of the sealed tube at ~40 µm FWHM at modest gain (~4 x 10^6). Despite the fixed pattern noise the images are stable, and the gain is quite uniform (Fig. 19) across the detector with multifiber edge gain deviations of the order 15%. The fast pulse signals measured at the MCP output face are essentially the same as standard MCPs, and fast timing data [18] taken with a similar configuration indicate <100 ps timing resolution is expected for single photons.

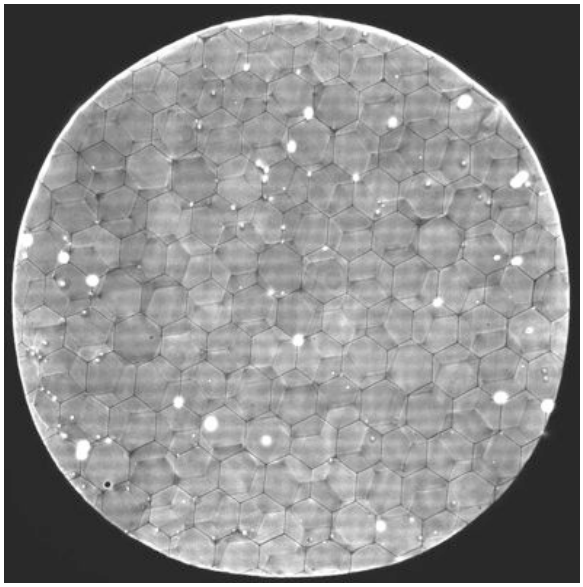


Fig. 17: 184nm UV illuminated image for 25mm opaque GaN ALD MCP sealed tube. MCP multifibers, and hotspots due to particulates are visible in the image.

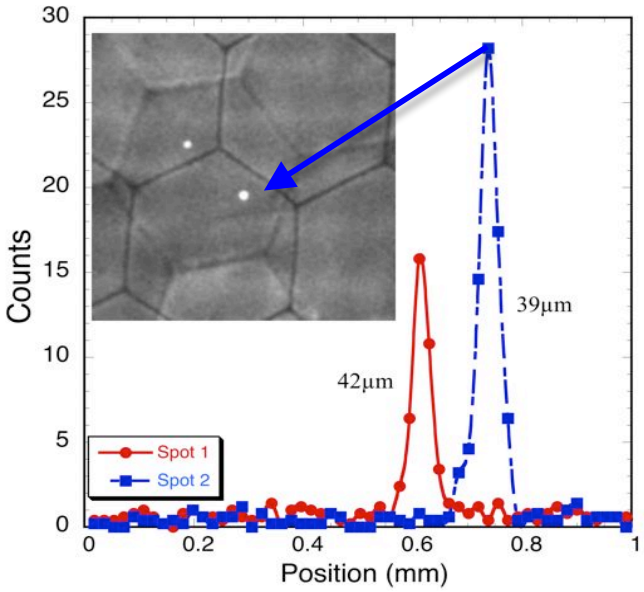


Fig. 18: Spatial resolution for the 25mm GaN ALD MCP tube shows ~40µm FWHM for bright spots, gain ~4 x 10^6. Both MCP hexagonal multifibers are also seen.

3.2 Planacon Tubes with Atomic Layer Deposited Borosilicate Substrate Microchannel Plates

To evaluate ALD MCPs as an alternative to standard MCPs we have begun evaluation of ALD borosilicate MCPs in a commercial sealed tube. The PHOTONIS Planacon provides a convenient format with a ~50mm active area (Fig. 14) to test basic functional parameters. The initial device uses a 32 x 32 anode pad array, and was fabricated with two 10 µm pore ALD MCPs having 60:1 l/d and 8° pore bias. The photocathode was a standard production bialkali, has efficiency (Fig. 21) close to the standard production expectations, and was measured four months after the tube was sealed. The uniformity of the cathode was also good with the lowest values at the extreme corners of the active area (Fig. 22), but much of the area was within 15% of the peak quantum efficiency value.

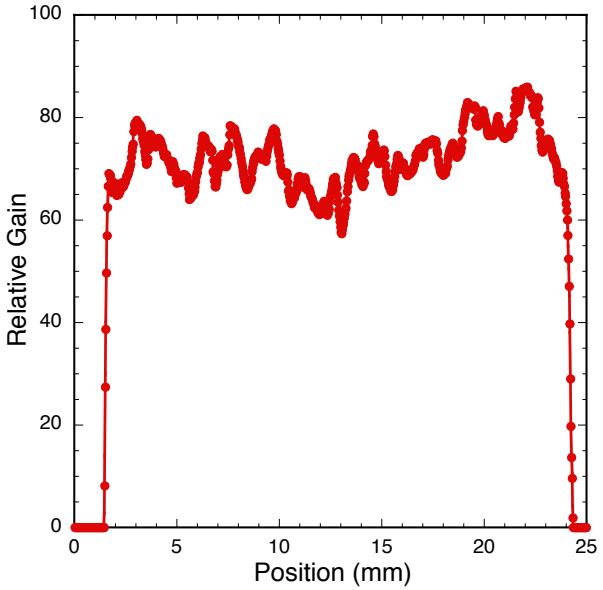


Fig. 19: Histogram of the average gain across the 25 mm opaque GaN ALD MCP sealed tube. Overall gain is flat to ~15%, features are due to the multifiber gain variations.

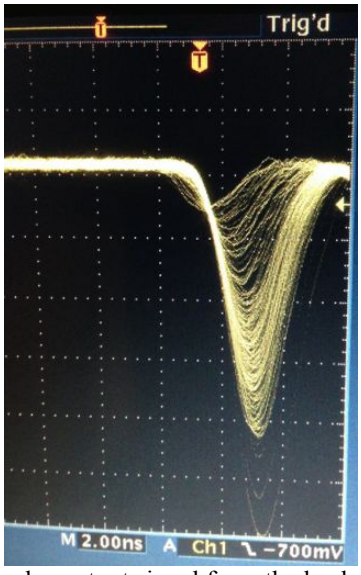


Fig. 20: Fast pulse output signal from the back of the MCPs of the 25 mm GaN ALD sealed tube using an Ortec VT120 amp. ~4 x 10^6 gain. 184 nm UV.

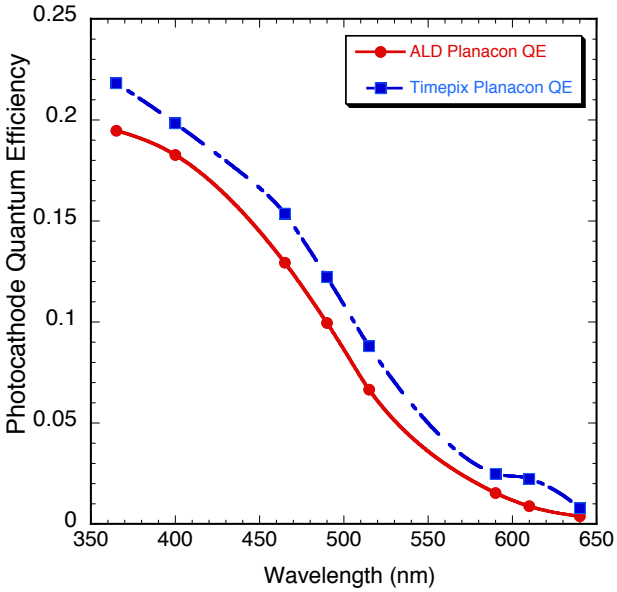


Fig. 21: Bialkali cathode quantum efficiency for a 50 mm Planacon with a pair of 53 mm, 10µm pore, 60:1 L/d, 8° bias ALD borosilicate substrate MCPs compared with a Timepix planacon [19] cathode quantum efficiency.

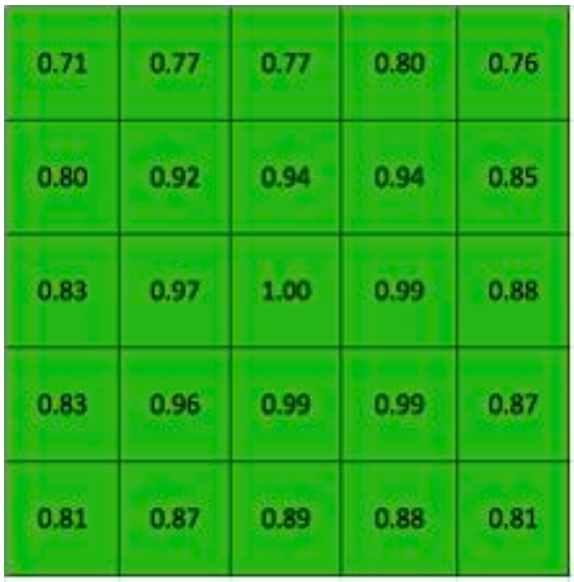


Fig. 22: Relative cathode quantum efficiency as a function of position, 50 mm bialkali cathode Planacon with ALD MCPs. 490 nm light.

The initial tests were done without the ability to perform 2D imaging, however this will be accommodated in the near future by coupling the planacon anodes to the preamplifier array used for the cross strip anode readout shown in Fig. 4. In the current tests we were however, able to use a 610 nm laser to investigate the pulse response and linearity of the detector. Fig. 23 shows the amplified output signals for laser pulses giving the equivalent of ~20 photoelectrons. The single photoelectron noise is seen at the baseline and is equivalent to a gain of ~5 x 10^5 with ~1300 V on each MCP. The laser pulse intensity was varied using neutral density filters (Fig. 24) down to the point where only single photoelectrons were produced. A more extensive set of tests, including those described here for other sealed tube devices will be performed with the fully integrated electronics in the near future. This will form a baseline for fabrication of more devices, and for future extensive testing including long term lifetests.

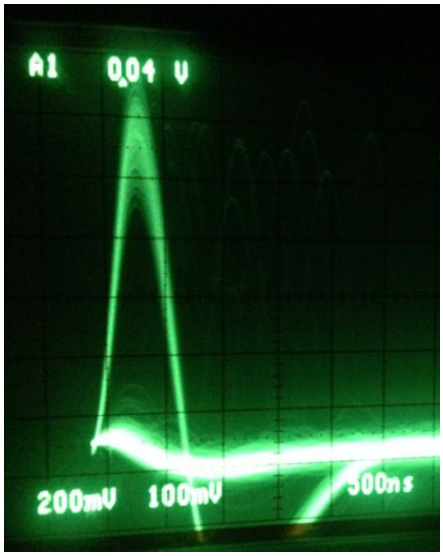


Fig. 23: 80 ps laser pulse giving ~20 e^- signals for a Planacon with a pair of 53 mm, 60:1 L/D, 10 µm pore borosilicate substrate ALD MCPs.

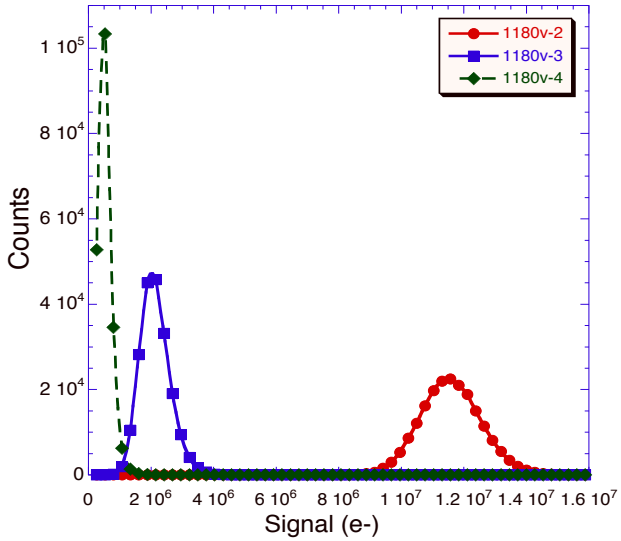


Fig. 24: 80 ps laser pulse signal amplitude distribution for a Planacon with a pair of ALD borosilicate substrate MCPs for 20e^- (2), 2e^- (3) & <1e^- (4) average per pulse.

4. ACKNOWLEDGEMENTS

We acknowledge the efforts of R. Raffanti, J. Tedesco, H. Frisch, PHOTONIS – (Roden, Brive & Lancaster), SVT Inc. and Incom Inc. for their assistance. This work was supported by NASA grants NNG11AD54G & NNX14AD34G.

5. REFERENCES

1. Siegmund, O.H.W., M.A. Gummin, J.M. Stock, et. al, Performance of the double delay line microchannel plate detect detectors for the Far-Ultraviolet-Spectroscopic Explorer, *Proc SPIE* 3114, pp.283-94 (1997).
2. Siegmund, O.H.W., P. Jelinsky, S. Jelinsky, et al., High resolution cross delay line detectors for the GALEX mission, *Proc. SPIE* 3765, pp.429-40 (1999).
3. Stock, J.M. O.H.W. Siegmund, J.S. Hull, et al., Cross-delay-line microchannel plate detectors for the Spectrographic Imager on the IMAGE satellite, *Proc SPIE* 3445, pp.407-14 (1998).
4. Siegmund, O.H.W., M.A. Gummin, T. Sasseen, et al., Microchannel plates for the UVCS and SUMER instruments on the SOHO satellite, *Proc. SPIE* 2518, pp.334-55 (1995).
5. Vallerga, J.; Zaninovich, J.; Welsh, B.; Siegmund, O.; McPhate, J.; Hull, J.; Gaines, G.; Buzasi, D. The FUV detector for the cosmic origins spectrograph on the Hubble Space Telescope, *Nuclear Instruments and Methods in Physics Research Section A*, Volume 477, Issue 1-3, p. 551-555 (2002).
6. Siegmund, O.H.W., J. McPhate, A. Tremsin, J.V. Vallerga, B.Y. Welsh and J.M. Wheatley, *AIP Conference Proceedings*, 984, 103 (2008).
7. Priedhorsky. W.and J. Bloch, *Applied Optics*, 44(3), 423-433 (2004).
8. Siegmund, O.H.W., J. Vallerga, P. Jelinsky, M. Redfern, X. Michalet, S. Weiss, "Cross Delay Line Detectors for High Time Resolution Astronomical Polarimetry and Biological Fluorescence Imaging", *IEEE* Nuclear Science Symposium and Medical Imaging Conference, (2005).
9. Michalet, X.; Siegmund, O. H. W.; Vallerga, J. V.; Jelinsky, P.; Millaud, J. E.; Weiss, S., Photon-counting H33D detector for biological fluorescence imaging, Nuclear Instruments and Methods, A, Vol. 567(1), p. 133 (2006).
10. Siegmund, O., J.V. Vallerga, A.S. Tremsin, J. McPhate, X. Michalet, S. Weiss, H.J. Frisch, R.G. Wagner, A. Mane, J. Elam, G. Varner. "Large Area and High Efficiency Photon Counting Imaging Detectors with High Time and Spatial Resolution for Night Time Sensing and Astronomy", Advanced Maui Optical and Space Surveillance Technologies Conference, (2012).
11. Siegmund, O.H.W. J.V. Vallerga, A. Tremsin, J. McPhate, B. Welsh "Optical Photon Counting Imaging Detectors with Nanosecond Time Resolution for Astronomy and Night Time Sensing" Advanced Maui Optical and Space Surveillance Technologies Conference Proceedings, p.E77 (2011).

12. Siegmund, O.H.W., J.B. McPhate, S.R. Jelinsky, J.V. Vallerga, A.S. Tremsin, R. Hemphill, H.J. Frisch, R.G. Wagner, J. Elam, A. Mane, "Large Area Microchannel Plate Imaging Event Counting Detectors With Sub-Nanosecond Timing," IEEE Transactions on Nuclear Science, 60(2), pp. 923-931 (2013).
13. Siegmund, O., N. Richner G. Gunjala, J.B. McPhate, A.S. Tremsin, H.J. Frisch, J. Elam, A. Mane, R. Wagner, C.A. Craven, M.J. Minot, *Proc. SPIE* 8859, 88590Y (2013).
14. Siegmund, O., J. McPhate, A.S. Tremsin, J.V. Vallerga, H.J. Frisch, R.G. Wagner, A. Mane, J. Elam, G. Varner. "Large Area flat panel Photon Counting Imaging Detectors for Astronomy and Night Time Sensing", Advanced Maui Optical and Space Surveillance Technologies Conference, (2013).
15. Mane. A. Q. Peng, J.W. Elam, D.C. Bennis, C.A. Craven, M.A. Detarando, J.R. Escolas, H.J. Frisch, S.J. Jokela, J. McPhate, M.J. Minot, O.H.W. Siegmund, J.M. Renaud, R.G. Wagner, and M. J. Wetstein "A novel atomic layer deposition method to fabricate economical and robust large area microchannel plates for photodetectors," Physics Procedia 37, 722 – 732 (2012).
16. Siegmund, O., Vallerga, J., Welsh, B., McPhate, J., Rogers, D. "High Speed Optical Imaging Photon Counting Microchannel Plate Detectors for Astronomical and Space Sensing Applications", Advanced Maui Optical and Space Surveillance Technologies Conference Proceedings. p.90 (2009).
17. Siegmund, O., Vallerga, J., Welsh, B., Tremsin, A., McPhate, J., "High Spatial resolution GaN and Optical Photon Counting Detectors with sub-nanosecond timing for Astronomical and Space Sensing Applications", Advanced Maui Optical and Space Surveillance Technologies Conference. p.69 (2008).
18. Adams, B; Elagin, A; Frisch, H; Obaid, R; Oberla, E; Vostrikov, A; Wagner, R; Wetstein, M. "Measurements of the gain, time resolution, and spatial resolution of a 20×20 cm^2 MCP-based picosecond photo-detector", Nuclear Instruments and Methods in Physics Research A, 732, p. 392-396 (2013).
19. Vallerga, J.; Tremsin, A.; DeFazio, J.; Michel, T.; Alozy, J.; Tick, T.; Campbell, M. "Optical MCP image tube with a quad Timepix readout: initial performance characterization", Journal of Instrumentation, 9(5), C05055 (2014).